Coaxial Noncontact Surface Compliance Distribution Measurement for Muscle Contraction Sensing

Masahiro Fujiwara* and Hiroyuki Shinoda†
The University of Tokyo

ABSTRACT

In this paper, we propose a coaxial noncontact surface compliance distribution measurement method for sensing human muscle contraction. Our measurement system is based on pressurization to a target object by acoustic radiation pressure and measuring of surface displacement. The directions of the ultrasound convergent beam and an optical beam for displacement measurement are identical in the proposed setup. This setup improves measurement accuracy especially for moving objects and bumpy surfaces. The effectiveness is examined by measuring human muscle compliance distribution for relaxed and contracted situations. This is the first evaluation of measurement time of human skin in vivo including moving situation.

Keywords: Hardness measurement, acoustic radiation pressure, ultrasound phased array, muscle contraction sensing.

Index Terms: Hardware—Communication hardware, interfaces and storage—Sensors and actuators

1 INTRODUCTION

In popular capturing systems, human motions are captured with visual-based methods for machine operation training, sports, medical surgery, and so on. However, the visual-based system misses force information which is often primary information for human activities and more important than the motion trajectory. Human physical activities can be described perfectly by the muscle contraction amount of the whole body in the given environment.

There also exist many human force measurement methods for observing human activities. The most straightforward method is to mount force sensors on the human hands or objects. Another approach is electromyography (EMG) which mounts electrodes on the human skin [1]-[6]. EMG estimates muscle contraction from measured electric potential on a skin and that does not require sensors on the hands contacting with the object.

For applying these methods, mounted sensors or electrodes on the skin are required. The human sometimes cannot move freely due to this constraint and they can be applied to only fixed and local areas on the human body practically. Especially for human-computer interface applications, it can be a critical problem that the human carries some special devices in advance.

We proposed a concept that noncontact surface compliance measurement system can detect muscle contraction using acoustic radiation pressure in WHC 2013 [7]. This system measures transition of muscle hardness which occurs when the muscle goes to contraction or relaxation [8].

In this paper, we examine the measurement errors and effect of the motion of the object, using an improved measurement system. The major improvement in the new system is that the ultrasound pressurization and optical measurement are coaxial as shown in Figure 1(a). This system achieves robust measurement for displacement noise and target surface motion by sharing a common axis for the pressurization and the displacement measurement. In experiments, required measurement time for human skin in vivo in a moving situation at a constant speed is evaluated.

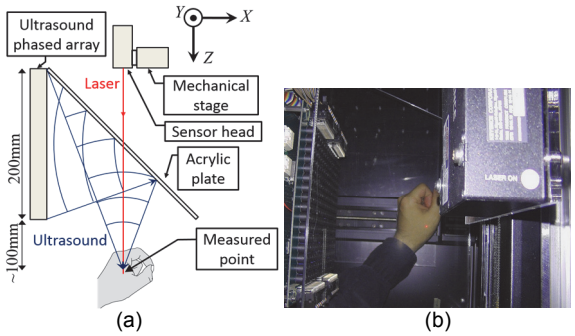

Figure 1: (a) Schematic diagram of coaxial setup of remote surface compliance measurement system. (b) Appearance of experimental setup.

2 COAXIAL SETUP OF NONCONTACT COMPLIANCE DISTRIBUTION MEASUREMENT

2.1 Noncontact Surface Compliance Distribution Measurement

Our method measures distribution of surface compliance defined as the ratio of vertical displacement at the center of the pressed area on a surface to the vertical force applied to the spot area. For supposing a situation that a human finger presses an object surface, the spot pressed area is about 1cm diameter circle as our previous work [7].

Measurement principle of our direct method has two steps: to press the object surface and to measure the displacement caused by pressing. The prototype system consists of an airborne ultrasound phased array for pressing and a laser displacement sensor (LK-G500, Keyence corp., Japan) for measuring displacement. The compliance distribution is obtained by scanning the pressing point and the displacement measuring point synchronously. The sensor is moved by an motorized mechanical stage (SGSP(CS)26-200(X), SIGMA KOKI CO., LTD., Japan) and the rate-limiting step of measuring time is the stage moving

Address: Faculty of Engineering Bldg. 14, 7-3-1 Hongo, Bunkyo-ku, Tokyo 113-8656, Japan.
*e-mail: masahiro_fujiwara@ipc.i.u-tokyo.ac.jp
†e-mail: hiroyuki_shinoda@k.u-tokyo.ac.jp

IEEE Haptics Symposium 2014
23-26 February, Houston, Tx, USA
978-1-4799-3131-6/14/$31.00 ©2014 IEEE

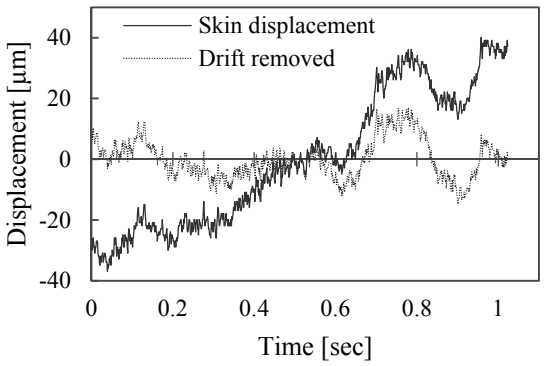

Figure 2: Involuntary movement of a fixed hand and movement after removing the linear drift of the involuntary movement.

time. The pressing point is electronically updated by an ultrasound phased array described below.

Noncontact pressurization is achieved by ultrasound acoustic radiation pressure [8][9]. The acoustic radiation pressure is non-zero bias of sound pressure proportioned to the sound energy. In the case of obliquely incident at an angle of θ to an object surface from air, magnitude of the acoustic radiation pressure P is represented as

$$P = 2E\cos^2\theta \tag{1}$$

where E is the acoustic energy density on the surface [10]. The acoustic energy density is proportional to the squared sound amplitude, and it is possible to press an object surface stationarily from a remote position. As a different point from air flow pressing, it is easy to press a small spot area on an object surface by using an ultrasound phased array.

An airborne ultrasound phased array [11] is used for generating converging ultrasound beam whose focal point is set at an object surface for pressurization. The ultrasound amplitude at the focal point is a summation of the amplitudes from all transducers on the phased array. Thus large acoustic radiation pressure occurs at the focal point according to Eq. (1). Due to the sufficiently large array aperture size, the focal diameter is comparable to the ultrasound wave length at a point around the phased array. The pressing point can be updated rapidly along an object surface. The updating time of the focal position is determined by control system performance. The actual updating time in this research within 1ms [11].

2.2 Evaluation of Minimal Measurement Time

The minimal measurement time for each point is limited by the SN ratio of displacement measurement and required accuracy. The measured RMS noise σ, which depends on the experimental environment, is less than 0.7 μm/$\sqrt{\text{Hz}}$ in our typical situation for a stationary surface.

If the measurement noise is white Gaussian noise, the pointwise measurement time T_{md} should satisfy

$$\sigma^2 / T_{\text{md}} \le \varepsilon^2, \tag{2}$$

for determining surface displacement ε, caused by the pressurization with a known waveform. Whole distribution measurement time T_{m} is represented as

$$T_{\text{m}} = N\,(\,T_{\text{md}} + T_0\,), \tag{3}$$

where N is the number of scanned points on a target surface, and T_0 is overhead time for each measurement that contains the motor stage movement time and the update time of the ultrasound focal position. In our experimental setup, the stage movement time is dominant since the movement speed is up to 4cm/s.

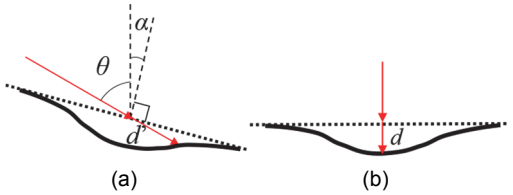

Figure 3: (a) Measured displacement d' for obliquely incident laser on a tilted surface.
(b) Measured vertical displacement d at the center of the deformation area for a horizontal surface.

For obtaining the best estimate ε in the given measurement time T_{m}, we use a quadrature detection of the displacement component for modulated ultrasound pressurization. Since the noise power spectrum is practically not white, the modulation frequency should be chosen in the frequency range with the lowest background displacement noise. In the case of a linear elastic object, the displacement frequency equals the ultrasound modulation frequency. Then the surface compliance is calculated as the ratio of displacement amplitude to the applied force amplitude. In the experiment, we choose 40Hz square wave pressurization because the background noise is small and the surface compliance frequency characteristics can be assumed to be flat with negligible phase delay for typical elastic surfaces. In the procedure of the displacement estimation, we removed the data drift as shown in Figure 2 before frequency analysis.

In the skin displacement measurement, both voluntary and involuntary motion of the skin should be considered. In this paper, we measure the human hand for (1) a stationary case where hand position is fixed voluntarily with involuntary vibrations and (2) a translational motion cases where the hand is intentionally moved laterally and vertically at constant speeds.

2.3 Coaxial Setup of Convergent Ultrasound and Displacement Measurement

Our method uses a triangulation-type laser displacement sensor for the robustness against the surface optical property variation. In previous method, there is a problem that the large laser incident angle magnifies the displacement measurement error. As shown in Figure 3(a), a measured displacement d' is based on the laser that was obliquely incident at an angle θ to the surface with an angle α inclined. The displacement d' is approximated as

$$d' \approx \frac{d}{\cos(\theta + \alpha)} \tag{4}$$

where d is the measured displacement of the surface for perpendicular incidence of the laser as shown in Figure 3(b).

We adopt a transparent acrylic plate to achieve the coaxial setup and maximizing the SN ratio. As shown in Figure 1(a), the sensor head measures displacement from just above the target surface through the acrylic plate. At the same time, the phased array is arranged perpendicularly to the target surface, and the generated ultrasound beam is reflected to the target surface by the acrylic plate. Traveling ultrasound wave in air is almost perfectly reflected by a solid flat surface and the spatial phase distribution is conserved relatively. Therefore by placing the transparent plate at an angle of 45 degrees with respect to the phased array, the phased array is virtually placed at the same position of the displacement sensor. The sensor is scanned by a mechanical stage while keeping the coaxial setup.

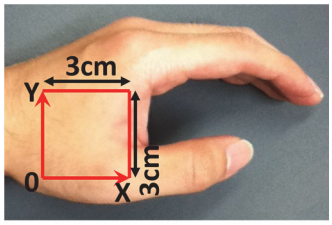

Figure 4: Measured area of surface compliance distribution on the left hand.

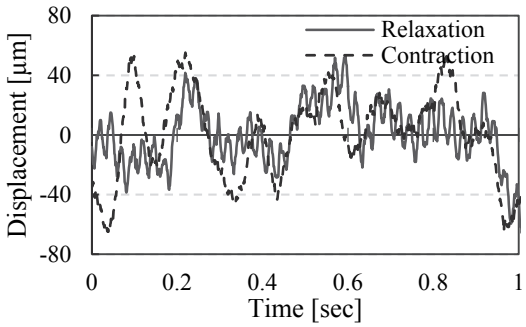

Figure 5: Measured displacement time series for relaxed and contracted muscle at (x, y) = (1.5cm, 1.5cm) shown in Figure 4 pressed by 40Hz ultrasound modulation. DC and linear bias are removed in the signal processing.

3 Experimental Results and Discussions

3.1 Experimental Setup

We perform two measurement experiments. First, we measure the muscle contraction distribution of a stationary hand for examining the measurement performance. Second, we evaluate the measurement time of the compliance for a moving hand to be related to the motion speed. For a fundamental evaluation, the experimental condition is limited to a particular posture in these experiments.

The implemented surface compliance measurement system consists of the ultrasound phased array and a laser displacement sensor as shown in Figure 1(a) and the appearance of the experimental set up is shown in Figure 1(b). Ultrasound transducers transmit 40kHz ultrasound and those are arranged in a 20cm × 20cm aperture. The minimal focal diameter is about 8.5mm, which is the wave length of the ultrasound. The acoustic radiation force at the focal point around 20cm distant from the array is about 17mN. The pushed spot area size is almost equal to the focal diameter. The measured objects are located at 20~30cm distant from the phased array virtually.

3.2 Measurement Experiments

The human skin surface compliance is measured by the proposed system. The measured area is between the bases of the thumb and index finger of the left hand as shown in Figure 4. Figure 5 shows measured displacement time series for the relaxed and contracted muscle at (x, y) = (1.5cm, 1.5cm) after removing the drift for 1.0 second measurement time at 1.00kHz sampling rate. The 40Hz vibration component is observed for the relaxed muscle. For the contraction state, the 40Hz vibration component is smaller than that of the relaxed state. Figure 6 shows the power spectrum of the measured displacement. The difference of the 40Hz component

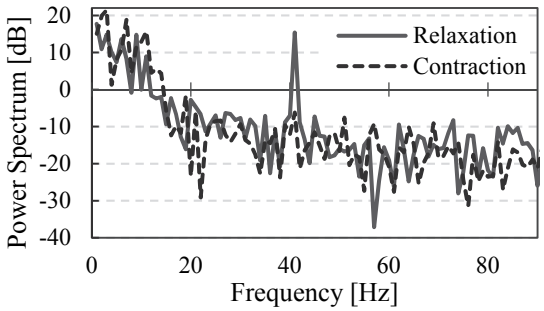

Figure 6: Power spectrum of the measured displacement shown in Figure 5.

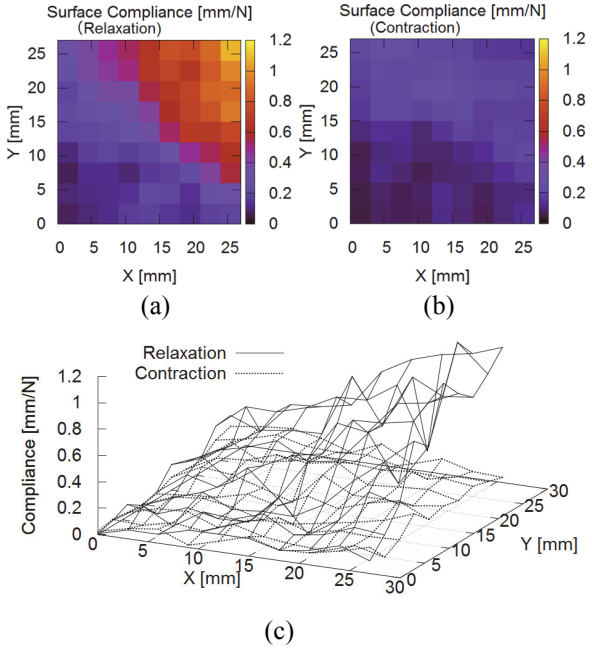

Figure 7: (a) 2D Map of measured surface compliance distribution for relaxed muscle. (b) 2D Map of the distribution for contracted muscle. (c) 3D plot of the distribution for contracted and relaxed muscle cases. .

power between these situations is more than 20dB for 1.0 second measurement time. And we found 1.0 second is necessary for obtaining 10dB SN ratio for the contraction state.

Figure 7(a), (b), and (c) show the surface compliance distributions of the measured area shown in Figure 4. The scanning of the measuring point by the mechanical stage is performed at 3mm intervals and the total measuring point number is 100 points. The observation time at each point is 1.0 second and the sampling rate is 1.00 kHz. In Figure 7(d), for the relaxation state drawn by solid lines, the large variation of compliance distribution is observed. For example, it is low compliance near the base of the thumb ($Y \approx 0$) and near the wrist ($X \approx 0$) because of bones under the skin area. The other area has high compliance up to about 1.2mm/N for relaxation state. On the other hand, for the contraction state drawn by broken lines, relatively small compliance (< 0.3mm/N) as a whole is observed. The compliance near the base of the thumb and wrist is low unchanged as the relaxation state. For the other area, the compliance is decreased from relaxation state up to about 1.0mm/N. These measurement

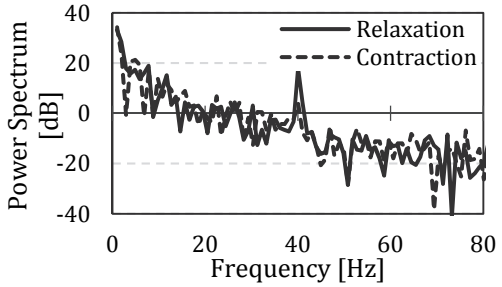

Figure 8: Power spectrum of the measured displacement at x = 1.5cm shown in Figure 4. The hand is moving in the y-direction for moving speed 1cm/s. T measurement point (x, y) = (1.5cm, 1.5cm) at t = 0 in the hand coordinate while the measuring point is fixed in the environment.

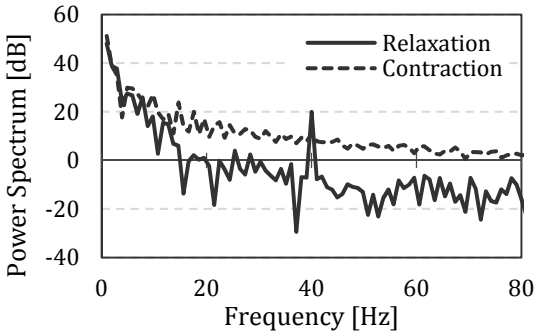

Figure 9: Power spectrum of the measured displacement at (x, y) = (1.5cm, 1.5cm). The hand moves upward vertically in the z-direction shown in Figure 1(a) at moving speed 1cm/s from the ultrasound focal point while the measuring point is fixed in the environment.

results reflect not only muscle contraction but also internal structure of the tissue such as bones.

3.3 Experimental Evaluation of Hand Motion Effect Compared to Previous Setup

Since the current system needs large measurement time, 1.0 second for sufficient SN ratio, the hand motion causes significant error. Figure 8 shows the power spectrum of the measured displacement at x = 1.5cm shown in Figure 4 for the moving hand in the y-direction at 1cm/s. The hand moves horizontally to moving distance 1cm from the point (x, y) = (1.5cm, 1.5cm) while the measuring point is fixed to the environment. The difference of the 40Hz component power between the contraction and relaxation situations is about 14dB. Figure 9 shows the power spectrum at (x, y) = (1.5cm, 1.5cm) for a moving hand in the z-direction at 1cm/s. The hand moves upward vertically by 1cm from the ultrasound focal point. The difference of the 40Hz component power between the contraction and relaxation situations is about 12dB. Figure 10 shows the measurement error of the compliance on the moving hand in the y-direction for relaxed hand. The measurement point shifts from (x, y) = (0, 0) to (0, Y [cm]) where $Y = vT_m$ and T_m = 1.0 second in the motion. We compare the two cases of the previous non-coaxial experiment setup and the current one. The experimental result shows 2mm/s is the acceptable speed for ensuring less than 0.1mm/N errors in the previous experimental condition. On the other hand, for the proposed coaxial setup, the acceptable speed is improved to 10mm/s. We need the further studies for generalizing the

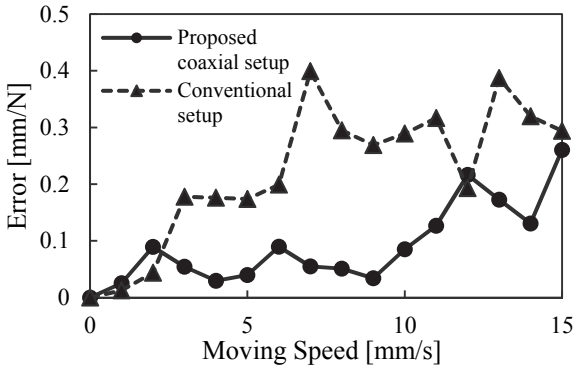

Figure 10: Measurement error of the compliance at the point (x, y) = (0, 0) at t = 0 on a moving relaxed hand in the y-direction.

improvement of the measurement. But a certain improvement is surely seen in this experiment.

4 Conclusions and Future Work

In this paper, we proposed a coaxial noncontact surface compliance distribution measurement method for sensing human muscle contraction. The proposed measurement system includes a transparent plate for reflecting convergent ultrasound beam and transmitting laser for displacement measurement. The required measurement time for human skin including moving situation is evaluated, using the improved system in this paper. The difference of the pressing frequency component of the displacement between contraction and relaxation states is about 20dB. For obtaining 10dB SN ratio for the hardest part in contracted state, we needed 1.0 second measurement time. Since the system requires such a relatively long measurement time, the hand motion causes a significant error. One possible solution for this error is to increase the radiation pressure and to implement a tracking system following the fixed measurement point on the skin.

Acknowledgments

This work was supported by JSPS KAKENHI Grant Number 25-9627.

References

[1] J. H. Lawrence and C. J. De Luca. Myoelectric signal versus force relationship in different human muscles. *Journal of Applied Physiology*, Volume 54, Number 6, pages 1653-1659, June 1983.

[2] P. A. Tesch, G. A. Dudley, M. R. Duvoisin, B. M. Hather, and R. T. Harris. Force and EMG signal patterns during repeated bouts of concentric or eccentric muscle actions. *Acta Physiologica Scandinavica*, Volume 138, Issue 3, pages 263-271, March 1990.

[3] L. Arendt-Nielsen and K.R Mills. The relationship between mean power frequency of the EMG spectrum and muscle fibre conduction velocity. *Electroencephalography and Clinical Neurophysiology*, Volume 60, Issue 2, pages 130-134, February 1985.

[4] L. Arendt-Nielsen, K.R Mills, and A. Forster. Changes in muscle fiber conduction velocity, mean power frequency, and mean EMG voltage during prolonged submaximal contractions. *Muscle & Nerve*, Volume 12, Issue 6, pages 493-497, June 1989.

[5] S. H. Westing, A. G. Cresswell, and A. Thorstensson, Muscle activation during maximal voluntary eccentric and concentric knee extension. *European Journal of Applied Physiology and*

Occupational Physiology, Volume 62, Issue 2, pages 104-108, 1991.

[6] P. V. Komi, V. Linnamo, P. Silventoinen, and M. Sillanpaa. Force and EMG power spectrum during eccentric and concentric actions. *Medicine and science in sports and exercise*, Volume 32, Issue 10, pages 1757-1762, 2000.

[7] M. Fujiwara and H. Shinoda, Noncontact Human Force Capturing based on Surface Hardness Measurement, *Proc. IEEE World Haptics Conference 2013*, Poster, pp.85-90, Daejeon, Korea, April 14-18, 2013.

[8] J. Awatani. Studies on Acoustic Radiation Pressure. I. (General Considerations). *Journal of the Acoustical Society of America*, Volume 27, pages 278-281, 1955.

[9] T. Hasegawa, T. Kido, T. Iizuka, and C. Matsuoka. A General Theory of Rayleigh and Langevin Radiation Pressures. *Acoustical Science and Technology*, Volume 21, Number 3, pages 145-152, 2000.

[10] M. Fujiwara and H. Shinoda. Remote Measurement Method of Surface Compliance Distribution for a Curved Surface Object. *In Proc. of SICE Annual Conference 2012*, pages 1-5, Akita, Japan, August 2012.

[11] T. Hoshi, M. Takahashi, T. Iwamoto, and H. Shinoda. Non-contact Tactile Display Based on Radiation Pressure of Airborne Ultrasound. *IEEE Transactions on Haptics*, Volume 3, Number 3, pages 155-165, 2010.

[12] M. Kaneko and T. Kawahara, CO-axis Type Non-contact Impedance Sensor. *in Proc. of the 2004 IEEE International Conference on Robotics & Automation*, New Orleans, LA, 2004.